ELSEVIER

Journal of Organometallic Chemistry 574 (1999) 155–162

Journal of Organometallic Chemistry

Decomposition of cyclopentadienyltricarbonylmanganese in highly vibrational excited states☆

Tetsuro Majima

The Institute of Scientific and Industrial Research, Osaka University, Mihogaoka 8-1, Ibaraki, Osaka 567-0047, Japan

Received 4 July 1998; received in revised form 6 August 1998

Abstract

Infrared multiple-photon decompositions (IRMPD) of cyclopentadienyltricarbonylmanganese and its methyl derivative (η^5-C_5H_4R)$Mn(CO)_3$ (R = H, CH_3) at 1045.02 cm^{-1} have been studied using a transversely excited atmospheric (TEA) CO_2 laser and compared with the UV photolysis and thermolysis. The main volatile products of the IRMPD at high laser fluences (200–400 J cm^{-2}) are CO and C_5H_5R both in the absence and presence of PF_3. On the other hand, (η^5-C_5H_4R)$Mn(CO)_2(PF_3)$ is obtained in the UV photolysis and thermolysis of (η^5-C_5H_4R)$Mn(CO)_3$ in the presence of PF_3. Therefore, the initial process in the IRMPD is found to be the dissociation of the Mn–cyclopentadienyl bond in contrast to that of the Mn–CO bond in the UV photolysis and thermolysis. The dissociation energy of the Mn–cyclopentadienyl bond is higher than that of the Mn–CO bond. The initial dissociation of the Mn–cyclopentadienyl bond in the IRMPD is confirmed with trapping of $Mn(CO)_3$ and cyclopentadienyl radicals by C_5H_5R, CO and isobutane. The Mn–cyclopentadienyl dissociation occurs through effective IR multiple-photon excitation of (η^5-C_5H_4R)$Mn(CO)_3$ to high vibrational states.

Keywords: Decomposition; Cyclopentadienyltricarbonylmanganese; Highly vibrational excited state

1. Introduction

Infrared multiple-photon decomposition (IRMPD) is a unique photochemical phenomenon because the decomposition occurs in highly vibrational excited states and in the electronic ground state [1]. Many studies on IRMPD have been done for rather simple molecules in relation to laser isotope separation. There are only two reports on IRMPD of organometallic compounds including a transition metal, i.e. the decomposition of transition metal carbonyls using a frequency-doubled TEA CO_2 laser at 5 μm, by Au et al. [2], and $Fe(CO)_5$ using an IR *p*-hydrogen Raman laser at 16 μm by Majima et al. [3].

Compared with the thermolyses and UV–vis photolyses, IRMPD of organometallic compounds including a transition metal has the following characteristics. It is possible to excite selectively a ligand chromophore or a metal–ligand bond, because the IR absorption bands are separated from each other. Thus, the selective excitation produces initially the ligand chromophore or the metal–ligand bond in highly vibrational excited states. However, the selective dissociation of the ligand chromophore or metal–ligand bond does not occur in the vibrational excited states, since the intramolecular vibrational relaxation proceeds faster than any unimolecular dissociation [1].

When several competitive processes are involved in a dissociation, the lowest energy process occurs more favorably than the high energy processes in a thermolysis [4]. On the other hand, the high energy process occurs predominantly at high laser fluences in IRMPD of many compounds, because the distribution of vibrational energy is localized to the high energy range in the excited states generated from infrared multiple-photon excitation (IRMPE) at high laser fluences [1,5]. Simi-

☆ Dedicated to the memory of the late Professor Rokuro Okawara.

0022-328X/99/$ - see front matter
PII: S0022-328X(98)00938-3

larly, it is expected that the high energy channel proceeds at high laser fluences in IRMPD of organometallic compounds. Therefore, the dissociation processes and the reactive intermediates in the IRMPD will be completely different from those in thermolysis.

In this work, the author has studied IRMPD of Mn complexes containing carbonyl (CO) and two different species of η^5-cyclopentadienyl (Cp) ligands, i.e. (η^5-C_5H_5)$Mn(CO)_3$ (CMT) and (η^5-$C_5H_4CH_3$)$Mn(CO)_3$ (MMT); see Scheme 1. The Cp ligands absorbs TEA CO_2 laser radiation in the 9–10 μm region, while both the CO ligand and Mn–CO bond do not. Therefore, the laser irradiation in the 9–10 μm region leads to the selective excitation of the Cp ligand in the CMT or MMT. The decomposition mechanism is compared with those in UV photolyses [6] and thermolyses [7] of CMT and MMT.

2. Experimental

2.1. Materials

CMT and MMT (Strem Chemicals, purity > 99%) were distilled in vacuum and degassed by several freeze pump–thaw cycles with dry ice/methanol to remove traces of carbon monoxides. Sulfur hexafluoride SF_6 (Asahi Glass Co.), trifluorophosphine PF_3 (Japan Oxygen Co.), Ar (Takachiho Trade Co.) were of the highest purity grades available from the manufacturer and used without further purification. Cyclopentadiene and methylcyclopentadiene were prepared by pyrolyses of dicyclopentadiene and methylcyclopentadiene dimer (Tokyo Kasei Co.), respectively. Cyclopentadiene and methylcyclopentadiene were purified by preparative GC.

2.2. IRMPD

The details of the experimental procedure of IRMPD have been described in previous papers [8,9]. Briefly, a TEA CO_2 laser beam passed through a 1.3 cm aperture and then was focused into a Pyrex reaction tube with a BaF_2 lens of 7.5 cm focal length. The laser fluences were calculated from the beam energy and size at the entrance window, focal length of the lens and beam divergence of 2×10^{-3} rad. The pulse width of the laser was 80 ns full width at half maximum (FWHM) without a tail (short pulse) or 80 ns FWHM with a 1.3 μs tail (long pulse). The repetition rate was 1.0 Hz. The cell has a 3-cm inner diameter, a 13-cm irradiation length, a 130-cm^3 internal volume (V_{cell}), a 9.4-cm^3 irradiated volume (V_{irr}) and KBr windows at both ends. The value of V_{irr} was calculated from the beam size at the entrance window, cell length and focal length of the lens. The irradiated sample was analyzed with an FT-IR spectrometer (Nicolet 5DXB), gas chromatograph (Shimadzu GC-7A and Hitachi 263-70), and quadruple mass spectrometer (NEVA TE-150). The energy absorbed from a laser pulse in CMT or MMT (E_{abs}) was measured by a photoacoustic technique [8b]. The number of absorbed photons per molecule ($\langle n \rangle$) is calculated from $\langle n \rangle = E_{abs}/Nhv$, where N is the number of molecules of CMT or MMT in the irradiated volume. The experimental set-up is shown in Fig. 1. After the irradiation, the reaction mixtures were analyzed with a FT-IR spectrometer, UV spectrometer, gas chromatograph and quadruple mass spectrometer. The yields of products were measured with GC-MS.

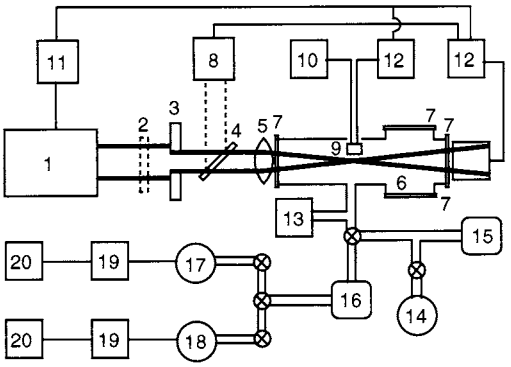

Fig. 1. Schematic diagram of the experimental set up. 1, TEA CO_2 laser; 2, attenuator; 3, aperture; 4, beam splitter; 5, BaF_2 lens; 6, reaction cell; 7, KBr window; 8, power meter; 9, microphone; 10, power supply; 11, pulse generator; 12, oscilloscope; 13, pressure gauge; 14, CMT or MMT; 15, vacuum pump; 16, Toepler pump; 17, condensable gas at −196°C; 19, gas chromatograph; 20, mass spectrometer.

A KrF excimer laser (Tachisto TACII system 100; pulse width of 20 ns, pulse energy of 5.8 mJ) and a low pressure Hg lamp (Arion Co. AL15GL19W) together with a rectangular quartz cell (pass length of 1.0 cm) were used for UV irradiation.

3. Results and discussion

3.1. Decomposition probability and products of the IRMPD

CMT and MMT have weak absorption bands in the 9–10 μm region assigned to the C–H bending and C–C stretching vibrations of the Cp ligands (Fig. 2) [10]. The

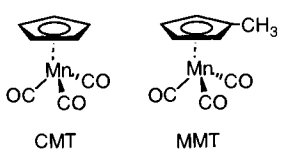

Scheme 1.

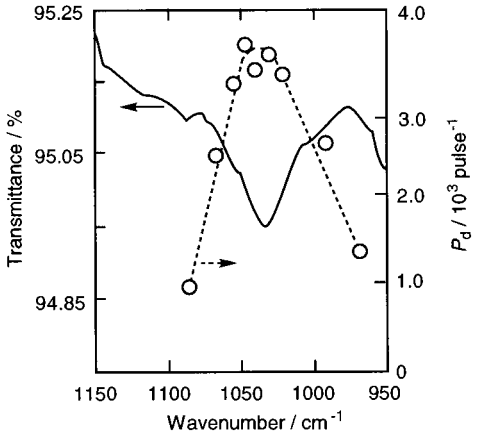

Fig. 2. IR spectrum of MMT (solid line) and plots (circles, broken line) of the decomposition probability (P_d) vs. the laser wavenumber (ν) in the short-pulsed IRMPD of MMT at laser fluence of 300 J cm^{-2} at the focus. Pressure of MMT, 47 mtorr.

absorption coefficient at the peak is 1.6×10^{-3} torr^{-1} cm^{-1}. IRMPD of CMT and MMT occurred when 47 mtorr of CMT and MMT were irradiated with the short pulse (pulse width, 80 ns FWHM) of 9P(22) line at 1045.02 cm^{-1} with the laser fluences of 240–400 J cm^{-2} at the focus.

The apparent decomposition fraction (k_d) is determined to be $k_d = 1.4 \times 10^{-4}$ pulse^{-1} from a plot of $-\ln(1-X)$ versus the number of laser pulses at low conversion, as shown in Fig. 3, where X = (pressure of consumed CMT or MMT)/(initial pressure of CMT or MMT). The decomposition probability (P_d) is given by $P_d = k_d V_{cell}/V_{irr}$, where V_{cell} and V_{irr} are the internal volume and the irradiated volume, respectively. The results are summarized in Table 1. The absorbed photons per molecule, 8.3, mean that one CMT or MMT molecule in the irradiated volume has an excess of vibrational energy of 24 kcal mol^{-1}, which is not enough to cleave a bond in CMT or MMT. It is clear that the energy of vibrational excited states is distributed over a wide range in the irradiated volume. CMT and MMT decompose when their vibrational energy is higher than the bond dissociation energies.

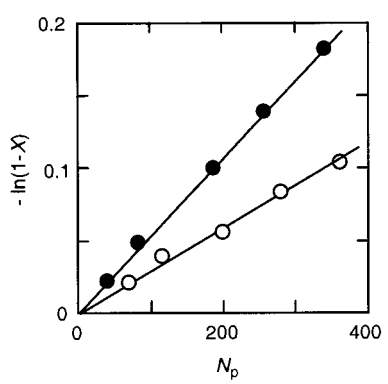

Fig. 3. Plots of $-\ln(1-X)$ vs. number of laser pulses (N_p) in the short-pulsed of IRMPD of CMT (circles) and MMT (solid circles), where X = (pressure of CMT or MMT)/(initial pressure of CMT or MMT). Pressure of CMT or MMT, 47 mtorr.

Table 1
Summary of IRMPD of CMT and MMT at high laser fluences (240–400 J cm^{-2})

Parameters and results	CMT	MMT
Pressure of starting gas (torr)	0.047	0.047
Absorption coefficient at laser wavenumber (torr^{-1} cm^{-1})	1.6×10^{-3}	1.6×10^{-3}
Absorbed photons per molecule	8.3	8.3
Decomposition fraction (pulse^{-1})	1.4×10^{-4}	2.7×10^{-4}
Decomposition probability (P_d) (pulse^{-1})	2.0×10^{-3}	3.8×10^{-3}
Product (yield/%)	CP (50) CO (210) $(C_5H_5)_2$ (<5) Others	MCP (37) CO (200) $(C_5H_4CH_3)_2$ (<5) Others
[CO]/[consumed CMT or MMT]	2.1	2.0

The absorption coefficient as well as the number of absorbed photons per molecule in CMT are almost equal to those in MMT, although k_d and P_d are slightly larger for MMT. The dissociation energy of Mn–Cp bond (D(Mn–Cp)) is reported to be 50.7 kcal mol^{-1} and the average dissociation energy of the Mn–CO bond (D(Mn–CO)$_{av}$) in CMT is 34.0 kcal mol^{-1} [11]. Since D of the first M–CO bond (D(Mn–CO)$_1$) is always the highest in non-substituted transition metal carbonyls (M(CO)$_n$) [8,11–14], D(Mn–CO)$_1$ in CMT is definitely higher than D(Mn–CO)$_{av}$. However, D(Mn–CO)$_1$ is lower than D(Mn–Cp), because the Mn–CO dissociation occurs initially in the thermolyses of CMT and MMT (vide infra). It has been reported by another group that D(Mn–Cp) is 71 kcal mol^{-1} higher than D(Mn–CO) [15]. The slightly higher P_d in MMT than in CMT is probably attributed to the slightly lower D(Mn–Cp) in MMT, because of the methyl substituent on the Cp ring.

The main volatile products were CO and cyclopentadiene (c–C_5H_6 (CP)) for CMT, and CO and methylcyclopentadiene (c-$C_5H_5CH_3$ (MCP)) for MMT. The ratios of CO and CP, or CO and MCP to CMT or MMT were 200–210% and 37–50%, respectively. Therefore, two CO ligands dissociate from one CMT or MMT molecule in average, whereas the Cp ligand dissociates to form CP or MCP in yields of 37–50%. Additionally non-volatile dimers of Cp ligands, $(C_5H_4R)_2$, were formed in low yields. These results show that CMT and MMT do not decompose completely into Mn, CO and Cp. In fact, non-identified products containing Mn, C, O and H atoms were found

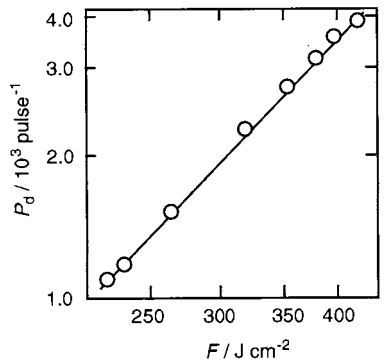

Fig. 4. Plots of P_d vs. laser fluence at the focus (F) in the short-pulsed IRMPD of MMT. Pressure of MMT, 47 mtorr.

as the minor products on the cell wall. The product analyses suggest that both Mn–CO and Mn–Cp bonds dissociate in the IRMPD of CMT and MMT.

3.2. Effect of laser fluence on the IRMPD

The dependence of P_d on the laser fluence at the focus (F) at 47 mtorr of MMT is shown in Fig. 4. P_d increased with an increase of F, in proportion to $F^{2.3}$, and also with an increase in the absorption coefficient at a given laser wavenumber as shown in Fig. 2. The decomposition was not observed for $F < 50$ J cm^{-2}. Fig. 5 shows that both MMT consumption and yields of MCP and CO per laser pulse increased with an increase of F (200–400 J cm^{-2}). From extrapolation to zero of the consumption and the yields, the threshold fluences were determined to be 150–170 J cm^{-2} for MMT consumption, CO formation and MCP formation. The nearly equal threshold fluences mean that one process of IRMPE occurs in the IRMPD of MMT. This result and the linear relationships of the consumption of MMT and yields of CO and MCP versus F suggest that the consumption of MMT and formation of products are explained by a common mechanism.

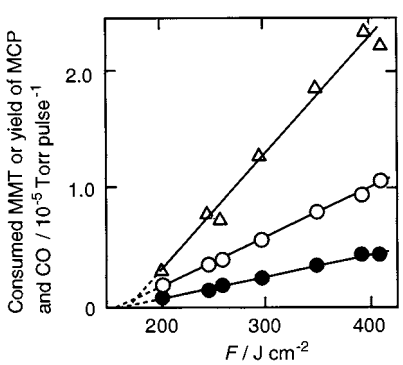

Fig. 5. Effects of F on consumed MMT (circles) or the yields of MCP (solid circles) and CO (triangels) per pulse in the short-pulsed IRMPD of MMT. Pressure of MMT, 47 mtorr.

3.3. Influence of PF_3 additive on the IRMPD

In order to elucidate the decomposition mechanism, the IRMPD of CMT and MMT in the presence of PF_3 have been studied. CO and CP, and CO and MCP were obtained in the short-pulsed IRMPD of CMT and MMT (50 mtorr) in the presence of PF_3 (3 torr) at $F = 200$–400 J cm^{-2}, which were similar to those in the short-pulsed IRMPD in the absence of PF_3 (Table 1). Since no PF_3-substituted complexes, such as (η^5-C_5H_4R)$Mn(CO)_{3-n}(PF_3)_n$ formed, the initial dissociation process in the short-pulsed IRMPD of CMT and MMT is suggested to be the dissociation of the Mn–Cp bond but not the Mn–CO bond.

The same experiment has been performed for MMT in the presence of PF_3 at $F = 180$–200 J cm^{-2}, which is slightly higher than the threshold fluences 150–170 J cm^{-2} for MMT. A trace amount of (η^5-C_5H_4R)$Mn(CO)_2(PF_3)$ was detected together with CO and MCP as the main products. This result shows that the Mn–CO bond dissociation also occurs as a minor dissociation process at $F = 180$–200 J cm^{-2} (low F), and that CMT and MMT in the high vibrational states decompose effectively, but CMT and MMT in low vibrational states do so but less efficiently. Consequently, the higher energy Mn–Cp dissociation occurs at high F, while the lower energy Mn–CO dissociation occurs as a minor process at low F. It is observed in IRMPD of various compounds that distribution of the vibrational energy and the branching ratio of the competitive processes depend on F [1,5,9]. The higher energy process occurs at high F, while the lower energy one occurs at low F.

The CO ligand exchange by PF_3 is well-documented in UV photolysis and thermolysis of transition metal carbonyls [16]. A PF_3-substituted complex in both UV photolysis and SF_6-photosensitized thermolysis [8a–c] of MMT was obtained in the presence of excess PF_3. The irradiation of a mixture of MMT and PF_3 (0.05 and 3 torr, respectively) with a low-pressure mercury lamp (19 W, 185 and 254 nm) or KrF laser (20 ns, 248 nm) gave (η^5-$C_5H_4CH_3$)$Mn(CO)_2(PF_3)$, (Mn–PF_3) as a main volatile product through electronic excitation (Eq. (1)), unimolecular decarbonylation (Eq. (2)) and substitution (Eq. (3)).

$$\mathrm{MMT} + h\nu \rightarrow \mathrm{MMT}^* \quad (1)$$

$$\mathrm{MMT}^* \rightarrow (\eta^5 - C_5H_4CH_3)Mn(CO)_2 + CO \quad (2)$$

$$(\eta^5 - C_5H_4CH_3)Mn(CO_2) + PF_3 \rightarrow (\eta^5 - C_5H_4\underset{(Mn\text{–}PF_3)}{CH_3})Mn(CO)_2(PF_3) \quad (3)$$

where the wavelength of light was 185–254 nm and * denotes electronic excitation.

The irradiation of a mixture of SF_6, MMT and PF_3 (0.5, 0.05 and 3 torr, respectively) with a short-pulsed

TEA CO_2 laser at 940.55 cm^{-1} and the laser fluence of 0.2 J cm^{-2}, without focusing of the laser beam, gave Mn–PF_3 through IRMPE of SF_6 (Eq. (4)), thermalization of all gaseous species to high local temperature (Eqs. (5) and (6)), unimolecular decarbonylation of MMT (Eq. (7)) and co-ordination of PF_3 (Eq. (3)).

$$SF_6 + nh\nu_1 \rightarrow SF_6^{\dagger} \quad (4)$$

$$SF_6^{\dagger} + A \rightarrow SF_6^{\ddagger} + A^{\ddagger} \quad (5)$$

$$MMT + A^{\ddagger} \rightarrow MMT^{\ddagger} + A \quad (6)$$

$$MMT^{\ddagger} \rightarrow (\eta^5 - C_5H_4CH_3)Mn(CO)_2 + CO \quad (7)$$

where $n > 1$, $\nu_1 = 940.55$ cm^{-1}; A = SF_6, MMT, PF_3; † and ‡ denote vibrational and thermal excitation, respectively.

Although the Mn–PF_3 was not produced in the short-pulsed IRMPD of CMT and MMT at high F (200–400 J cm^{-2}), Mn–PF_3 was detected in the short-pulsed IRMPD at low F (180–200 J cm^{-2}), in the long-pulsed (pulse width, 1.3 μs) IRMPD in the presence of PF_3, together with the products of the short-pulsed IRMPD at high F. Similarly, Mn–PF_3 was also detected in the short-pulsed IRMPD of a mixture of CMT–PF_3 or MMT–PF_3 in the presence of Ar (70 torr).

3.4. Mechanism of the IRMPD

On the basis of the experimental results including trapping of intermediates by additives as described below, the following decomposition mechanism is shown for the short-pulsed IRMPD of CMT and MMT at high F in Eqs. (8)–(12):

$$(\eta^5 - C_5H_4R)Mn(CO)_3 + mh\nu_2 \rightarrow (\eta^5 - C_5H_4R)Mn(CO)_3^{\dagger} \quad (8)$$

$$(\eta^5 - C_5H_4R)Mn(CO)_3^{\dagger} \rightarrow [c - C_5H_4R]^{\bullet} + {}^{\bullet}Mn(CO)_3 \quad (9)$$

$$[c - C_5H_4R]^{\bullet} + AH \rightarrow c - C_5H_5R + A \quad (10)$$

$${}^{\bullet}Mn(CO)_3(+\text{others}) \rightarrow CO + \text{other products} \quad (11)$$

$$2[c - C_5H_4R]^{\bullet} \rightarrow (C_5H_4R)_2 \quad (12)$$

where $m > 1$, $\nu_2 = 1045.02$ cm^{-1}; AH = CMT or MMT; R = H, CP; R = CH_3, MCP.

The irradiation of CMT or MMT with the strong short-pulsed 10 μm radiation at high F excited CMT or MMT to high vibrational states through the C–C stretching and the C–H bending modes of the Cp ring (Eq. (8)). The initial process is the Mn–Cp dissociation to form c-C_5H_4R and $Mn(CO)_3$ radicals ([c-C_5H_4R]$^{\bullet}$ and $^{\bullet}Mn(CO)_3$, respectively) (Eq. (9)). [c-C_5H_4R]$^{\bullet}$ successively abstracts a hydrogen atom from CMT, MMT or dissociation products to yield C_5H_5R (Eq. (10)). Similarly, $^{\bullet}Mn(CO)_3$ decomposes successively into CO and Mn as main products, and forms non-volatile compounds containing Mn, C, O and H atoms in part (Eq. (11)). Radical coupling of [c-C_5H_4R]$^{\bullet}$ occurs to produce $(C_5H_4R)_2$ in a low yield (Eq. (12)). From the nearly equal threshold fluence for MMT consumption, CO formation and MCP formation (Fig. 5), it is suggested that the secondary processes of [c-C_5H_4R]$^{\bullet}$ and $^{\bullet}Mn(CO)_3$ radicals occur without further excitation because of the high internal energy in the radicals, or that secondary IRMPE of [c-C_5H_4R]$^{\bullet}$ and $^{\bullet}Mn(CO)_3$ radicals occurs within a laser pulse. It is found that the pre-exponential factor of Arrhenius parameters is important compared with the activation barrier in IRMPD of various compounds [1,5], while the activation barrier is the predominant factor in thermolyses. It is suggested that the pre-exponential factor for the Mn–Cp dissociation seems to be larger than that for Mn–CO dissociation, and therefore, the Mn–Cp dissociation predominantly occurs in the vibrational excited CMT† and MMT† localized in the higher energy range.

Contrary to the initial Mn–Cp dissociation in the short-pulsed IRMPD of CMT and MMT at high F, the initial process is the Mn–CO dissociation in the long-pulsed IRMPD and in the short-pulsed IRMPD in the presence of excess Ar. Even in the short-pulsed IRMPD at low F, the Mn–CO dissociation occurs as a minor process together with the Mn–Cp dissociation as the major process. Intramolecular and/or intermolecular redistributions of vibrational energy of CMT† or MMT† occur to give CMT§ and MMT§ in equilibrated vibrational states during IRMPE of the Cp ligand in the short-pulsed IRMPD at low F, in the long-pulsed IRMPD, and in the short-pulsed IRMPD in the presence of Ar (Eq. (13)). Since the distribution of vibrational energy in CMT§ and MMT§ is not localized in the higher energy range as in CMT† or MMT†, the lower energy Mn–CO dissociation occurs initially in CMT§ and MMT§ (Eq. (14)).

$$(\eta^5 - C_5H_4R)Mn(CO)_3^{\dagger} + A \rightarrow (\eta^5 - C_5H_4R)Mn(CO)_3^{\S} + A^{\S} \quad (13)$$

$$(\eta^5 - C_5H_4R)Mn(CO)_3^{\S} \rightarrow (\eta^5 - C_5H_4R)Mn(CO) + CO \quad (14)$$

where A = MT, MMT, Ar; § denotes vibrational excitation.

3.5. Trapping of intermediate radicals by additives

In order to confirm the initial dissociation process of the Mn–Cp bond and intermediates of Cp$^{\bullet}$ and $^{\bullet}Mn(CO)_3$ radicals, the products in the short-pulsed IRMPD of a mixture of CMT–MCP or MMT–CP were examined. Although CP or MCP itself decomposed by IRMPD, P_d of CP and MCP was two orders of magnitude smaller than that of CMT or MMT. The

short-pulsed irradiation of a mixture of CMT and MCP (0.047 and 1.0 torr, respectively) with $F = 240–400$ J cm^{-2}, gave MMT as well as CO and CP as main volatile products. The ratios of CO, CP and MMT yields per consumed CMT were 1.6, 0.52 and 0.13, respectively. The yield of CO decreased with an increase of yield of CP. Similarly, the short-pulsed irradiation of a mixture of MMT and CP (0.047 and 1.0 torr, respectively, $F = 200–400$ J cm^{-2}) gave CMT together with CO and MCP. The ratios of CO, MCP and CMT yields per consumed MMT were 1.5, 0.61 and 0.11, respectively.

On the other hand, the substitution of the Cp ligand by CP or MCP did not occur in UV photolyses nor SF_6-photosensitized thermolyses of CMT–MCP or MMT–CP mixtures, in which substitution of a CO ligand by CP or MCP was observed to form (η^5-Cp)Mn(CO)$_2$(η^2-CP) or (η^5-Cp)Mn(CO)$_2$(η^2-MCP), respectively [17].

The results eliminate not only Mn–CO dissociation but also step-wise substitution of η^5-Cp by CP or MCP through (η^3-C_5H_4R)(η^2-c-C5H5R)Mn(CO)$_3$ or (σ-C_5H_4R)(η^4-c-C_5H_5R)Mn(CO)$_3$ as the initial process. It is clearly suggested that the initial Mn–Cp dissociation gives Cp and $^{\bullet}$Mn(CO)$_3$ radicals (Eq. (9)). In the short-pulsed IRMPD of the CMT–MCP mixture, [c-C_5Hs]$^{\bullet}$ abstracts a hydrogen atom from MCP and gives CP and [c-$C_5H_4CH_3$]$^{\bullet}$ (Eq. (15)). Recombination of [c-$C_5H_4CH_3$]$^{\bullet}$ and $^{\bullet}$Mn(CO)$_3$ yields MMT (Eq. (16)). Alternatively, $^{\bullet}$Mn(CO)$_3$ reacts with MCP to yield MMT and H (Eq. (17)), while CP is formed by reaction of [c-C_5H_5]$^{\bullet}$ and H (Eq. (18)).

$$[c-C_5H_5]^{\bullet} + \mathrm{MCP} \rightarrow \mathrm{CP} + [c-C_5H_4CH_3]^{\bullet} \quad (15)$$

$$[c-C_5H_4CH_3]^{\bullet} + {}^{\bullet}\mathrm{Mn(CO)_3} \rightarrow \mathrm{MMT} \quad (16)$$

$$^{\bullet}\mathrm{Mn(CO)_3} + \mathrm{MCP} \rightarrow \mathrm{MMT} + \mathrm{H} \quad (17)$$

$$[c-C_5H_5]^{\bullet} + \mathrm{H} \rightarrow \mathrm{CP} \quad (18)$$

The CMT formation in the short-pulsed IRMPD of the MMT–CP mixture can be explained by similar processes.

Next, the products in the short-pulsed IRMPD of CMT or MMT, in the presence of isobutane, $(CH_3)_3CH$, are examined. The short-pulsed irradiation of a mixture of CMT and isobutane (0.047 and 1.0 torr, respectively) with $F = 240–400$ J cm^{-2} gave CO, CP and isobutene, $(CH_3)_2C{=}CH_2$, as the main volatile products. The ratios of CO, CP and isobutene yields per consumed CMT were 1.2, 0.85 and 0.40, respectively. The yield of CP increased with a decrease of yield of CO, and was nearly two times the yield of isobutane. Similarly, the short-pulsed irradiation of a mixture of MMT and isobutene (0.047 and 1.0 torr, respectively, $F = 200–400$ J cm^{-2}) gave CO, MCP and isobutene with the ratios of 1.3, 0.78 and 0.38 per consumed MMT, respectively.

The results clearly indicate that the initial Mn–Cp dissociation gave Cp and $^{\bullet}$Mn(CO)$_3$ radicals (Eq. (9)). In the short-pulsed IRMPD of the CMT (or MMT) and isobutane mixture, [c-C_5H_4R]$^{\bullet}$ abstracts a hydrogen atom from isobutane to give CP (or MCP) and t-butyl radical (Eq. (19)). Disproportionation of the t-butyl radical gives isobutene and isobutane (Eq. (20)).

$$[c-C_5H_4R]^{\bullet} + (CH_3)_3CH \rightarrow c-C_5H_4R + (CH_3)_3C^{\bullet} \quad (19)$$

$$2(CH_3)_3C^{\bullet} \rightarrow (CH_3)_3CH + (CH_3)_2C{=}CH_2 \quad (20)$$

In order to trap $^{\bullet}$Mn(CO)$_3$, the products in the short-pulsed IRMPD of CMT or MMT (0.047 torr) in the presence of excess CO (10 torr) at $F = 240–400$ J cm^{-2} were examined. Mn$_2$(CO)$_{10}$ was detected as a minor product together with CP or MCP as the main product. This result clearly shows that coupling of $^{\bullet}$Mn(CO)$_3$ occurs in the presence of excess CO to give Mn$_2$(CO)$_{10}$ as a stable product (Eq. (21)).

$$2\ {}^{\bullet}\mathrm{Mn(CO)_3} + 4\mathrm{CO} \rightarrow \mathrm{Mn_2(CO)_{10}} \quad (21)$$

3.6. Initial dissociation of Mn–Cp bond in the IRMPD

The Mn–CO dissociation occurs initially in the thermolyses, because of D(M–CO) < D(Mn–Cp) [11,15]. Moreover, a Cp ligand is stable kinetically toward other ligand molecules, such as CP and MCP, although a Cp ligand converts sometimes into η^3-C_5H_4R or σ-C_5H_4R [18]. On the other hand, the Mn–Cp dissociation occurs initially in the short-pulsed IRMPD of CMT and MMT through the selective excitation of the Cp ligand at high F to vibrational excited CMT† and MMT† localized in higher energy range. The lower energy Mn–CO dissociation occurs as a minor process at low F, since intramolecular energy redistribution occurs rapidly during IRMPE to give CMT† and MMT† localized in not only higher but also lower vibrational energy ranges. When intramolecular and intermolecular energy redistribution proceeds rapidly during IRMPE, the Mn–CO dissociation occurs initially in the long-pulsed IRMPD and in the short-pulsed IRMPD in the presence of Ar.

The influence of a massive central metal atom on dissociation of the organometallic compounds has been studied by two groups. Rogers et al. reported that a thermal reaction of a fluorine atom and tetraallyl tin leads to the formation of $CH_2{=}CHF$ and (allyl)$_3$Sn–CH_2 at a rate being approximately 10^3 times faster than that estimated from the RRKM theory. The non-RRKM behavior was explained by the effect of heavy tin atom blocking vibrational energy transfer from the chemically activated allyl to the other allyl groups [19]. Lopez and Marcus studied the influence of a heavy mass barrier on intramolecular energy transfer for linear chain C–C–C–Sn–C–C–C on the basis of

classical trajectory calculations [20], and concluded that the non-RRKM behavior is expected when a ligand chromophore of organometallic compounds having a heavy metal atom is selectively excited to high vibrational states by IRMPE.

The mass of a Mn atom is 55, which is much heavier than those of C, H and O atoms of Cp and CO ligands, but Mn atom is not as big as the tin atom. Therefore, the Mn atom cannot block intramolecular energy transfer from the Cp ligand in vibrational excited states to CO ligands in vibrational ground state, and intramolecular V–T/R processes proceed much faster than any unimolecular dissociation processes [1,4,5]. Consequently, the initial Mn–Cp dissociation (Eq. (9)) occurs after intramolecular energy redistribution of the vibrationally excited CMT or MMT in high vibrational states at high F.

It may be interesting to discuss a possibility of the quasi-atomization mechanism in the IRMPD of CMT or MMT at high F, where $CMT^{\dagger}$ or $MMT^{\dagger}$ decompose directly into η^5-$C_5H_4R + Mn + 3CO$. The fragments decompose successively or react with molecules in the cell into final products, or recombined to give (η^5-C_5H_4R)Mn, (η^5-C_5H_4R)Mn(CO), (η^5-C_5H_4R)-$Mn(CO)_2$, ($\eta^5C_5H_4R$)$Mn(CO)_3$, or $^{\bullet}Mn(CO)_3$ during cooling the process of the reaction mixture. If so, ($\eta^5C_5H_4R$)$Mn(CO)_{3-n}(PF_3)_n$ could be produced in the IRMPD of CMT or MMT in the presence of PF_3. The rates of the fragment recombinations to return back to the starting CMT or MMT and to give stable products must be slow because of low concentrations of the fragments and high reaction orders of the fragment recombinations of η^5-C_5H_4R, Mn and three CO. Observation of exchange of η^5-C_5H_4R ligands in CMT–MCP and MMT–CP mixtures and formation of $Mn_2(CO)_{10}$ in the presence of CO may not be consistent with the quasi-atomization mechanism, while the initial Mn–Cp dissociation of $CMT^{\dagger}$ or $MMT^{\dagger}$ seems to be reasonable for the IRMPD mechanism.

It should be noted that the short-pulsed IRMPD of CMT or MMT at high F is the first example of metal–Cp dissociation for organometallic compounds containing Cp and CO ligands, and that highly co-ordinatively unsaturated species such as $^{\bullet}Mn(CO)_3$ are produced as intermediates. The highly co-ordinatively unsaturated species are of current interest with respect to their structures, bonds and reactivities. Although such species can not be produced by thermal or one-photon excitation of organometallic compounds, the IRMPD is a method that produces them. Since only a few studies have been reported on IRMPD of organometallic compounds, the characteristics are not well-established. As can be seen in the IRMPD of CMT and MMT, IRMPD of organometallic compounds has potential to provide new reaction pathways that have not been found in the usual thermal and photochemical reactions.

Although it is established that intramolecular vibrational energy transfer occurs faster than any unimolecular dissociation in IRMPD of various compounds [1,4,5], it is still open for discussion whether the selective excitation leads to the specific dissociation of the ligand or metal–ligand bond in IRMPD of organometallic compounds including the central metal atom having a large mass. It is important to study IRMPD of various organometallic compounds including a massive metal atom and a variety of ligands.

4. Conclusions

The initial process of the short-pulsed IRMPD of CMT or MMT at high F is the Mn–Cp dissociation in CMT or MMT in high vibrational excited states, generated from the selective IRMPE of the Cp ligand and fast intramolecular energy redistribution of the vibrationally excited CMT or MMT in high vibrational states. The author is currently studying IRMPD of other organometallic compounds to clarify the mechanism and to find new reaction processes through selective excitation of a ligand to high vibrational states.

Acknowledgements

The author would like to thank Professor Shigeyoshi Arai, Dr Michio Takami and Professor Tadahiro Ishii for their useful discussion and Dr Shigeru Ishikawa for his assistance in the experiments, since this work was partly performed at The Institute of Physical and Chemical Research, 2-1 Hirosawa Wako-shi, Saitama, 351-0198, Japan. This work was partly supported by a Grant-in-Aid for Scientific Research (Nos. 09226223, 10132237, 09450319 and 09875209) from the Ministry of Education, Science, Sport and Culture of Japan.

References

[1] For reviews, see: (a) J.I. Steinfeld, Laser Induced Chemical Processes, Plenum Press, New York, 1981. (b) V.S. Letokhov, Non-Linear Laser Chemistry, Springer, Berlin, 1983. (c) D.W. Lupo, M. Quack, Chem. Rev, 87 (1987) 181. (d) V.S. Letokhov, Appl. Phys. B46 (1988) 237.

[2] M.-K. Au, P.A. Hackett, M. Humphries, P. John, Appl. Phys. B33 (1984) 65.

[3] T. Majima, H. Tashiro, K. Midorikawa, M. Takami, Chem. Phys. Lett. 121 (1985) 65.

[4] (a) R.J. Robinson, K.A. Holbrook, Unimolecular Reactions, Wiley-Interscience, New York, 1972. (b) S.W. Benson, Thermochemical Kinetics, Wiley-Interscience, New York, 1976.

[5] (a) A.S. Sudobo, P.A. Schulz, E.R. Grant, Y.R. Shen, Y.T. Lee, J. Chem. Phys. 70 (1970) 912. (b) J. Troe, J. Chem. Phys. 73 (1980) 3205. (c) A.C. Baldwin, J.R. Barker, J. Chem. Phys. 74 (1983) 3823.

[6] P.J. Giordano, M.S. Wrighton, Inorg. Chem. 16 (1977) 160.
[7] R.J. Angelici, W. Loewen, Inorg. Chem. 6 (1967) 682.
[8] (a) T. Majima, T. Ishii, T. Matsumoto, M. Takami, J. Am. Chem. Soc. 111 (1989) 2417. (b) T. Majima, Y. Matsumoto, M. Takami, J. Photochem. Photobiol. A Chem. 71 (1993) 213–219. (c) T. Majima, Co-ord. Chem. Rev. 132 (1994) 141. (d) T. Majima, T. Miyahara, K. Haneda, M. Takami, Jpn. J. Appl. Phys. 33 (1994) L223. (e) T. Majima, T. Miyahara, K. Haneda, T. Ishii, M. Takami, Jpn. J. Appl. Phys. 33 (1994) 4759. (f) T. Majima, T. Miyahara, K. Haneda, M. Takami, J. Photochem. Photobiol. A Chem. 80 (1994) 423.
[9] (a) T. Majima, K. Sugita, S. Arai, Chem. Phys. Lett. 163 (1989) 29. (b) T. Majima, T. Ishii, S. Arai, Bull. Chem. Soc. Jpn. 62 (1989) 1701. (c) T. Majima, T. Ishii, S. Arai, Bull. Chem. Soc. Jpn. 63 (1990) 728.
[10] (a) R.M. Silverstein, G.C. Bassler, Spectrometric Identification of Organic Compounds, Wiley, New York, 1967. (b) K. Nakamoto, Infrared and Raman Spectra of Inorganic and Coordination Compounds, Wiley, New York, 1978.
[11] J.R. Clipperfield, J.C.R. Sney, D.E. Webster, J. Organomet. Chem. 178 (1979) 177.
[12] P.C. Engelking, W.C. Lineberger, J. Am. Chem. Soc. 101 (1979) 5569.
[13] I.M. Waller, J.W. Hepburn, J. Chem. Phys. 88 (1988) 6658.
[14] K.E. Lewis, D.M. Golden, G.P. Smith, J. Am. Chem. Soc. 106 (1984) 3905.
[15] J.A. Connor, Topics Current Chem. 71 (1977) 71.
[16] R.J. Clark, M.A. Busch, Acc. Chem. Res. 6 (1973) 246.
[17] E.O. Fischer, M. Herberhold, Essays in Co-ordination Chemistry, Birkhaeuser, Basel, 1965, p. 259.
[18] (a) F.A. Cotton, T.J. Marks, J. Am. Chem. Soc. 91 (1969) 7281. (b) A.E. Smith, Inorg. Chem. 11 (1972) 165.
[19] P. Rogers, D.C. Montague, J.P. Frank, S.C. Tyler, F.S. Rowland, Chem. Phys. Lett. 89 (1982) 9.
[20] V. Lopez, R.A. Marcus, Chem. Phys. Lett. 89 (1982) 231.